Direct Focused Ion Litography of Biphasic Calcium Phosphate (BCP) Bioceramics Surfaces

Feray Bakan[1], Melike Çokol Çakmak[2], Meltem Sezen[1], Elif Çelik[2], Zaeema Khan[2]

[1]Sabanci University, Nanotechnology Research and Application Center, Istanbul, Turkey
[2]Sabanci University, Faculty of Engineering and Natural Sciences, Istanbul, Turkey

Abstract

Because the calcified tissues of mammalians are made up of calcium phosphate (CaP), several compounds of synthetic CaPs are widely used in orthopedic applications for many targets. These include repairment and reconstruction of bone tissue defects; bone fracture healing; strengthening dental tissues and as the coatings for implant materials owing to their excellent biocompatibility and bioactivity. The interface between the orthopedic implant and the surrounding host tissue may play a significant role on the clinical aspect. Expected effects are usually bony ingrowth (osseointegration), stimulation of osteogenesis (osteoinduction), increased vascularization, and improved mechanical stability. Among these factors, surface texture or nano/micro-topography of an implant material can drastically alter the interaction between the implant and the cell. Therefore, examining cell behavior has crucial importance depending on the surface texture of the substrates. Among all lithography techniques, Focused Ion Beam (FIB) based direct ion lithography is a convenient and practical way in order to form nano and micro structures in desired sizes and geometries.

In this study, biphasic calcium phosphate (BCP) surfaces were modified using a dual-beam platform (FIB-SEM) and the cell interaction of mammalian osteoblast-like cells (MG-63) on the related surfaces was investigated *in-vitro*. Repeating patterns of square, circle and line-array ion-milled structures and square carbon deposition layers (10x10 μm) were formed on BCP pellet surfaces at the FIB. Cell-surface interaction was then observed both using Fluorescence Microscopy and high-resolution SEM imaging. Besides, Fluorescence microscopy images were analyzed by using ImageJ software to obtain qualitative information on cell adhesion behavior on the structured surface of BCP. This study showed that surface topography of the bioceramic substrates at the nano and micro scale contribute to the cell adhesion behavior.

1. Introduction

Nowadays, taking an important part in the health sector and improving the life quality, biomaterials have high-added and hence high financial value. Calcium phosphate compounds are widely used as bone graft material in tumor surgery and bone fracture healing, to strengthen dentin in dentistry and as a coating material for implants. BCP is a calcium phosphate biomaterial which contains an intimate mixture of hydroxyapatite (HA), $Ca_{10}(PO_4)_6(OH)_2$, and beta-tricalcium phosphate (beta-TCP), $Ca_3(PO_4)_2$ at different ratios and is obtained by sintering the calcium deficient hydroxyapatite at temperatures of 700°C and above [1]. Since BCP contains a stable apatite phase (HA) and a more soluble/biodegradable phase (β-TCP) together, it is promising for many medical applications. BCPs are commercially used to control the solubility and strength of an artificial bone [1].

On the other hand, the use of high resolution electron microscopes provides precise and certain results for discipline-free applications in science and technology. In particular, Focused Ion Beam (FIB) Microscopy enables simultaneous structuring and characterization skills down to nanometer scale, including; site specific analysis, ion milling, deposition, micromachining, prototyping and manipulation. In this study, FIB-SEM dual-beam platforms were used for performing direct ion-milling and carbon deposition processes in order to form micron-sized array geometries locally and in the desired shape and geometries.

In this work, BCP pellet surfaces were structured via direct ion-lithography and the cell interaction of the osteoblast-like cells on the related surfaces are investigated *in vitro*. The adhesion behavior was observed using complementary imaging techniques, e.g. SEM and Fluorescence Microscopy observations.

2. Experimental Procedure

2.1 Preparation of BCP

BCP nanoparticles were synthesized by water-based sol-gel technique, which was applied according to a similar procedure, formerly reported by Bakan et al. [2]. $Ca(NO_3)_2.4H_2O$ and $NH_4H_2PO_4$ were used as the Ca and P precursors, respectively, with a Ca/P molar ratio of 1.55. Both precursors were prepared using 18.2 MΩ cm deionized water. The pH of both solutions was adjusted with ammonia. The Ca precursor was added dropwise to the P precursor with a peristaltic pump at a constant volumetric rate of 3 mL/min at room temperature. The ultimate gel was stirred at room temperature for 48 h. After aging, precipitated particles were collected by filtration and were then washed with deionized water to remove impurities. The filter cake was then dried for 12 h in a vacuum oven at 40°C and the nanoparticles were subsequently obtained. The nanoparticles were first pressed at 5 tons with a single axis press in order to form a 7 mm diameter pellet. Afterwards, two-step sintering process was carried out to complete the chemical conversion of BCP formation. The sintering was done at 750ºC for 2 h followed by 0.5 h at 1000ºC. After sintering, the particles were left for cooling inside the oven.

2.2 Characterization of Nanoparticles and Pellet Surfaces

To analyze the phase composition of the particles, X-ray diffraction (XRD) analysis was carried out by a Bruker AXS Advance D8 using CuK radiation at the step scanning mode, applying a tube voltage of 40 kV and a tube current of 40 mA. A step size of 0.02◦ and a scan speed of 1◦/min were applied. In addition, Raman Spectroscopy measurements were done using Renishaw Raman InVia System coupled with a 532 nm green laser, for identifying the chemical groups that are present in the BCP sample. The morphology of the particles was characterized using a JEOL-JEM-2100F UHR7HRP Transmission Electron Microscopy (TEM). The roughness and 3D topography of the BCP pellet surfaces were investigated by Atomic Force Microscopy (AFM) with a Bruker Multi-Mode AFM system.

2.3. Nanostructuring by Direct Ion Lithography

For nanostructuring, the produced BCP pellets were subjected to direct ion milling and gas assisted ion-beam-induced deposition in a JEOL JIB 4601F MultiBeam FIB-SEM platform. Surface modification processes were carried out by exposing Ga^+ ions directly onto BCP ceramic surfaces and by diverting the storage gas (carbon) which is sprayed through gas injection system (GIS) to a targeted surface simultaneously with the application of ion bombardment. The dimensions of the patterns were optimized according to the sizes of the cells that were chosen in this study. Since the nuclei of MG-63 cells have an average diameter of 20 µm, the arrays of 10x10 µm square patterns and 10 µm Ø circle patterns were prepared on BCP pellet surfaces. Line arrays had an interspacing of 10 µm.

2.4 Cell Culture on Modified Surfaces

The human osteoblast-like cell line, MG-63, was purchased from the American Type Culture Collection, ATCC. Cell culture was maintained in Dulbecco's Modified Eagle's Medium (DMEM) supplemented with 10% fetal bovine serum, 1% L-glutamine, 1% non-essential amino acids (NEAA) and 1% penicillin/streptomycin. The cells were maintained in a humidified incubator with 5% CO_2 at 37°C. Until confluency, the cells were passaged at a 1:4 split ratio approximately twice a week. Experiments were performed using the cells after the tenth passage**.** For the passaging, the cells were washed with PBS and incubated with trypsin-EDTA for 5 min at 37°C to detach cells from the flasks.

The MG-63 cells were seeded on BCP pellets with a density of 10^4 cells/cm^2 for each pellet. Cells were grown on BCP pellets for 24, 48 and 72 h to observe the cell adherence to patterned and non-modified (as a control) surfaces.

2.5 Immunofluorescence and Cytoskeletal Observation

MG-63 cells were cultured on BCP pellets at 37°C in 5% CO_2 humidified atmosphere. After 2 days of culture, cells were washed with PBS and fixed with 4 % (w/v) paraformaldehyde in PBS buffer for 10 minutes at room temperature. The samples were then washed with distilled water three times for 5 min and permeabilized with 0.1% Triton X-100 at room temperature for 10 min. Following the washing with distilled water, DAPI was added to stain the nucleus of the MG-63 cells. Then the pellets were observed under both Inverted Fluorescence Microscope and SEM.

3. Results and Discussion

3.1 Characterization of BCP

Figure 1 shows the XRD diffractogram of the BCP nanoparticles. The X-ray diffraction patterns of BCP were identified with the Joint Committee on Powder Diffraction Standards (JCPDS) cards (00-09-0432 for HA and 00-09-0169 for β-TCP). Phase analysis revealed that all major peaks of HA and β-TCP were present in the spectrum. Figure 2 shows the Raman spectrum of the sintered BCP nanoparticles. All bands have been assigned to internal vibrational

modes of the phosphate groups. The strong peak at 960 cm^{-1} is assigned to the totally symmetric stretching mode (υ1) of the tetrahedral PO_4^{-2} group (P–O bond) [3-4]. Triple degenerate bending mode (υ4) of the PO_4 group (O–P–O bond) was observed at 593 cm^{-1} and 581 cm^{-1} [4-6] Triple degenerate asymmetric stretching mode (υ3) of the PO_4^{-2} group (P–O bond) was observed at 1048 cm^{-1} [5-6].

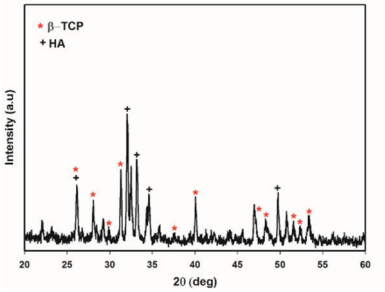

Figure 1. XRD spectrum of the sintered BCP.

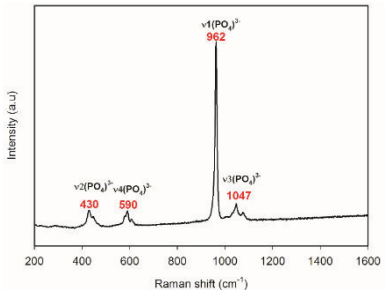

Figure 2. Raman spectrum of the sintered BCP.

Bright field TEM micrograph is given in Figure 3. BCP particles show a rod-like morphology of approximately 15 nm diameter and 100 nm length.

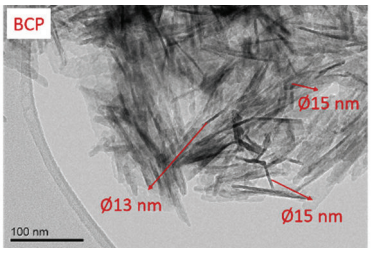

Figure 3. Bright filed TEM image of the BCP nanoparticles.

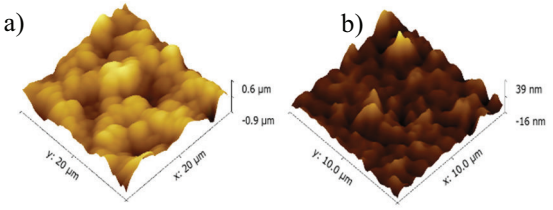

Figure 4. AFM 3D topography images of the BCP surface a) before FIB milling b) after FIB milling.

To investigate the effect of the patterning processes on the surface roughness and morphology, AFM analysis was done on untreated and treated surfaces (Figure 4). After FIB milling, the surface roughness decreased, and relatively smoother surfaces were obtained.

3.2 Surface modifications by FIB-SEM platform

SE-SEM images of ion-milled structures (a-c) and ion beam induced carbon deposition (d) on BCP surface are shown in Figure 5 and Figure 6.

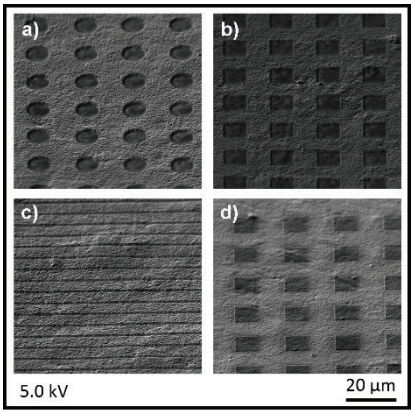

Figure 5. SE-SEM micrographs: (a) circle milling, (b) square milling, (c) array milling and (d) square deposition.

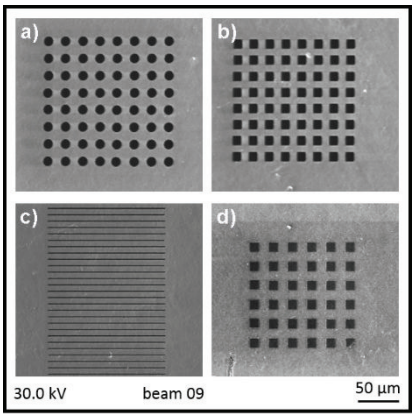

Figure 6. SE images generated by ions: a) circle milling, (b) square milling, (c) array milling and (d) square deposition.

3.3 *In vitro* analysis of surface-cell interactions

The effect of surface structuring on cell adhesion was observed by using MG-63 osteosarcoma mammalian cell line. Cell nuclei and actin filaments of MG-63 cells are clearly visible in fluorescence microscope as they are stained with DAPI and phalloidin stains (Figure 7). The BCP surfaces were left to incubate with cells for 24h, 48h, and 72h (Figure 8). As the incubation time increases, the oval to spindle shape of the cells became more triangular. They also had more contact with each other after 48 h of incubation.

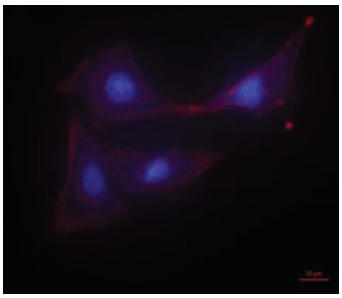

Figure 7. Fluorescence Microscopy image of MG-63 cells cultured on BCP surface. Scale bar is 20 µm.

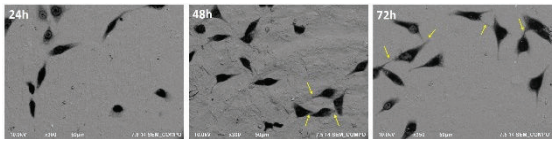

Figure 8. BSE-SEM images of MG-63 cells on BCP surfaces under different incubation durations.

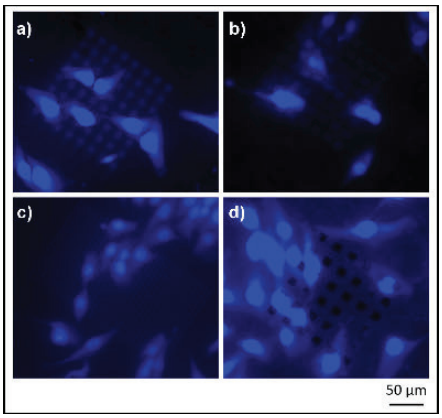

Figure 9. Fluorescence Microscopy images of MG-63 cells adhered on the structured BCP surfaces after 24h incubation.

According to the Fluorescence Microscopy images given in Figure 9, the number of MG-63 cells that were counted by Image J Software showed a distribution related to the patterns that were formed on the BCP surfaces. This distribution is given in Figure 10. The results show that the accumulation of the cells is more likely to form on the square deposition patterns compared to the rest.

4. Conclusion

In this study, controlled nano/micro structuring of BCP surfaces were carried out using ion lithography at the FIB-SEM. The effect of surface topography characteristics play an important role in determining cell adhesion and accumulation behavior. This study also verifies the practical use of FIB-SEM platforms for the prototyping of nano/micro structures on hard biomaterials.

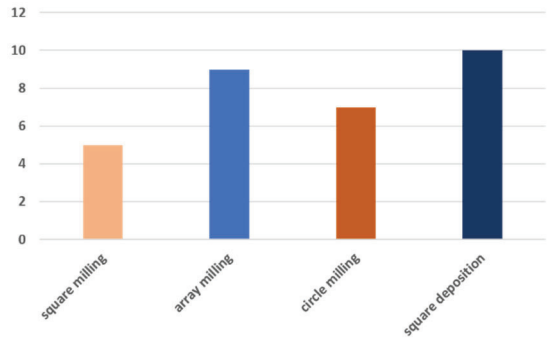

Figure 10. Number of cells in ROI (counted via Image J Software)

Acknowledgment

The authors would like to thank The Scientific Research Council of Turkey (Grant No: 115M788) and COST CM-1301 for providing financial support.

5. References

[1] LeGeros RZ, Lin S, Rohanizadeh R, Mijares D, LeGeros JP. Biphasic calcium phosphate bioceramics: preparation, properties and applications. Journal of materials science: Materials in Medicine. 2003 Mar 1;14(3):201-9.

[2] Bakan F, Kara G, Cakmak MC, Cokol M, Denkbas EB. Synthesis and characterization of amino acid-functionalized calcium phosphate nanoparticles for siRNA delivery. Colloids and Surfaces B: Biointerfaces. 2017 Oct 1;158:175

[3] O'shea DC, Bartlett ML, Young RA. Compositional analysis of apatites with laser-Raman spectroscopy:(OH, F, Cl) apatites. Archives of Oral Biology. 1974 Nov 1;19(11):995-1006.

[4] Griffith, WP. 1970. "Raman studies on rock-forming minerals. Part II. Minerals containing MO3, MO4, and MO6 groups", J Chem Soc (A) ,286–291.

[5] De Aza, PN., Guitian, F., Santos, C., De Aza, S., Cusco, R., Artus, L., 1997. "Vibrational investigation of calcium phosphate compounds 2. Comparison between hydroxyapatite and β-tricalcium phosphate", Chem Mater,9, 916–922.

[6] Sauer, GR., Zunic, WB., Durig, JR., Wuthier, RE., 1994. "Fourier transform Raman spectroscopy of synthetic and biological calcium phosphates", Calcif Tissue Int, 54, 4.